ISSN: 0067-2904

Assessing the Effect of Fe_2O_3 Nanoparticles on Catalase Activity in Patients with Chronic Periodontitis: *In Vitro* study and Molecular Docking

Sara A. Hatem[1], Zaizafon N. Nasif [1]*, Eaman A. S. Al-Rubaee[2]
[1]*Department of Chemistry, College of Science, Mustansiriyah University, Baghdad, Iraq*
[2]*Department of Basic Sciences, College of Dentistry, University of Baghdad, Iraq*

Received: 10/11/2022 Accepted: 17/6/2023 Published: 30/7/2024

Abstract

Periodontal disease, also known as gum disease, is a chronic inflammatory condition that affects the supporting structures of the teeth, including the gums and underlying bone. It is primarily caused by a bacterial infection resulting from poor oral hygiene practices. The main objectives of the current study were to synthesize iron oxide nanoparticles (Fe_2O_3-NPs) and their characteristics were analyzed through UV, SEM, and X-ray analysis. Additionally, the dispersion of the synthesized NPs was investigated using UV and TEM techniques. The study also aimed to assess the kinetic behavior and the impact of Fe_2O_3-NPs on catalase activity in the saliva of the patient and control groups. The findings revealed a significant increase in catalase activity ($p>0.05$) in both serum and saliva of all patient groups compared to the control group. The UV-visible spectrum shows that the absorption peaks for synthesized α- and γ-iron oxide nanoparticles was at 225 nm. According to the SEM image analysis, the primary particle size of the nano-particles is approximately 26.8 nm. The X-ray diffraction results indicate that the Fe_2O_3-NPs range in size from 14 nm to 26 nm. UV and TEM study conclude that water a suitable solvent for Fe_2O_3-NPs dispersion on kinetic study of catalase (CAT) activity. The kinetic data cleared that the α-Fe_2O_3-NPs have an inhibitory effect for the total activity of salivary CAT in the samples of both healthy and patients with chronic periodontitis. Lineweaver–Burk graph showed that (α-Fe_2O_3) inhibit catalase by un comp. inhibition. γ-Fe_2O_3-NPs inhibited total salivary CAT activity in healthy and patients with chronic periodontitis samples. Lineweaver –Burk graph showed that (γ-Fe_2O_3) inhibit catalase by uncompetitive inhibition.

Keywords: Catalase, iron oxide nanoparticles, Chronic Periodontitis, enzyme inhibition, saliva.

تقدير تأثير الدقائق النانوية لأوكسيد الحديديك على فعالية الكاتلاز في مرضى التهاب اللثة المزمن: دراسة مختبرية ودوكنك

سارة عبد الناصر حاتم[1]، زيزفون نبيل نصيف[1]*، إيمان علي سلمان الربيعي[2]
[1]قسم الكيمياء, كلية العلوم, الجامعة المستنصرية, بغداد, العراق
[2]فرع العلوم الأساسية, كلية طب الأسنان, جامعة بغداد, بغداد, العراق

*Email: violetrose_iniraq@yahoo.com

الخلاصة

يعد التهاب اللثة والمعروف أيضاً بمرض gum حالة التهابية مزمنة تؤثر على التراكيب الداعمة للأسنان بما في ذلك اللثة والعظم أسفل الأسنان. تعد عدوى البكتريا الناتجة عن عادات النظافة السلبية المسبب الرئيسي للمرض. هدفت هذه الدراسة الى تخليق جزيئات أكسيد الحديد النانوية Fe_2O_3–NPs والتوصيف مع تحليل الأشعة فوق البنفسجية ، SEM والأشعة السينية. دراسة تشتت الجزيئات النانوية من أكسيد الحديد المركب باستخدام الأشعة فوق البنفسجية و TEM. وايضاً هدفت الدراسة الى دراسة حركية وتأثير جزيئات أكسيد الحديد النانوية على نشاط الكاتلاز في لعاب المرضى والأصحاء. أظهرت النتائج أن هناك زيادة معنوية في فعالية الكاتلاز ($p> 0.05$) في كل مجموعة المرضى في مصل الدم واللعاب مقارنة مع الأصحاء. يوضح الرسم البياني المرئي للأشعة فوق البنفسجية أن قمم الامتصاص للجسيمات النانوية المكونة من أكسيد الحديد ألفا وبيتا كانت عند 225 نانومتر. تُظهر صورة SEM أن حجم الجسيمات الرئيسية للجسيمات النانوية يبلغ حوالي 26.8 نانومتر. يُظهر حيود الأشعة السينية أنه تم العثور على Fe_2O_3–NPs في حدود 14 نانومتر – 26 نانومتر. خلصت دراسة UV و TEM إلى أن الماء مذيب مناسب لتشتت Fe_2O_3–NPs في الدراسة الحركية لنشاط الكتلاز. أوضحت البيانات الحركية أن α–Fe_2O_3–NPs لها تأثير مثبط للنشاط الكلي للكتلاز اللعابي في عينات كل من الأصحاء والمرضى المصابين بالتهاب دواعم السن المزمن. أظهر الرسم البياني Lineweaver–Burk أن (α–Fe_2O_3) يثبط الكاتلاز بواسطة بشكل لا تنافسي. تثبط γ–Fe_2O_3–NPs إجمالي فعالية الكتلاز اللعابي في الأصحاء والمرضى الذين يعانون من عينات التهاب دواعم السن المزمن. أظهر الرسم البياني Lineweaver –Burk أن (γ–Fe_2O_3) يثبط الكاتلاز عن طريق تثبيط غير تنافسي.

1. Introduction

Periodontal disease, which is highly prevalent, affects approximately 80% of the global population and is the leading cause of dental decay. The most common forms of periodontal diseases are plaque-induced gingivitis and periodontitis. Periodontal disease refers to an inflammatory pathological condition that affects the gum and bone support (periodontal tissues) surrounding the teeth [1].

There are two types of periodontal diseases: Gingivitis, which is characterized by inflammation of the gums at the neck of the teeth, and Periodontitis, which involves inflammation of the bone and tissues supporting the teeth. Gingivitis is the initial stage of gum disease and is commonly found in adults. It is a reversible form of periodontal disease that does not cause damage to the connective tissue or bone [2].

Gingivitis can be caused by plaque (bacterial) or non-plaque factors (such as viral infections or allergies), although plaque is the most common cause. Both chronic and acute forms of gingivitis exist. Acute gingivitis can be attributed to specific pathogens, bacteria, or trauma. Chronic inflammation of the gum tissues surrounding the teeth is often associated with the bacterial biofilm (plaque) that forms on the teeth and gums [3].
Periodontitis, which is the term for periodontal disease when it affects the bone and surrounding tissue, is characterized by the development of pockets or gaps between the tooth and the gums [4].

Results from intra-oral and radiographic testing, such as sample of blood on probing (BOP), probing pocket depth (PPD), clinical attachment level (CAL), alveolar bone, and flexibility of the tooth, are used to determine the presence of periodontitis [5, 6].Takahara has discovered the lack of catalase in the blood (acatalasemia), and possibly also in tissue (acatalasia). The deficiency was therefore called the disease of Takahara. A progressive oral gangrene resulting from H_2O_2-generating bacteria [7].

Many species of catalases are thought to have 60–65 k Da tetrameric complex, with each monomer containing an I X fe–protoheme molecule (4 heme groups per tetramer). Human catalases are tetrameric structures that include four units of firmly bonded NADPH. Although this molecule does not thought to be necessary for the enzyme's ability to convert hydrogen peroxide to water and oxygen, it does prevent catalase from being inactivated by hydrogen peroxide. With an ideal pH range of 6.8 to 7.5, catalase has the highest rate of turnover of all the catalysts. The enzyme can act in two ways: catalytically, turning H_2O_2 into decomposition products (α-phase), or peroxidatively, via oxidization alcohols, format or nitrate (β-phase) and removing H_2O_2. Catalase decomposes H_2O_2 into water and molecular oxygen without free radical production [7].

The vanguard of nanotechnology's explosive development is nanoparticles (NPs). These substances are necessary and exceptional in several spheres of human life due to their unique size-dependent characteristics [8]. Iron oxides are often common, frequently utilized because they are cheap, and essential in many geophysical and ecological operations. They are also widely utilized by people, such as haemoglobin, coatings, paints, and lasting dyes (such as those used in colored concrete and thermite) [9]. Magnetite (Fe_3O_4), maghemite (γ-Fe_2O_3), and hematite (α-Fe_2O_3) are the most 3 species of iron oxide that have been found naturally occurring. For the magnetic isolation of biochemical components and cells as well as the magnetic guiding of particle assemblies for site-specific drug administration, iron oxide NPs were initially utilized in biological sciences and thereafter in pharmacy [10]. Due to its use in diagnostic and therapeutic procedures, magnetic carriers and particles have seen an increase in clinical uses over the past few decades [11, 12]. The aim of this study was to synthesize two phases of iron oxide nanoparticles (α-Fe2O3-NPs and γ-Fe2O3-NPs) using the photolysis method. The main objective of the study was to investigate the in vitro effects of α-Fe2O3-NPs and γ-Fe2O3-NPs on the activity of catalase in patients with chronic periodontitis. The focus was on exploring the potential biochemical applications of these nanoparticles and their impact on catalase activity, which is relevant to understanding their potential therapeutic effects in the context of chronic periodontitis.

2. Materials and Methods

2.1 Sample collection

Unstimulated saliva and serum samples were collected from a group of 60 patients with chronic periodontitis, aged between 20 and 45 years, as well as from 28 normal patients, also aged between 20 and 45 years. The samples were obtained from the teaching hospital of the College of Dentistry at the University of Baghdad during the time frame of 10:00 a.m. to 11:00 a.m. Patients and volunteers with osteoporosis, osteomalesia, cardiovascular disease, renal failure, hypertension alcoholics and smokers were excluded from the study.

2.2 Determination of salivary and sera catalase activity

The evaluation of catalase in the specimens was conducted using the method developed by Goth et al. This technique involves intricate reactions with ammonium molybdate to quantitatively measure the unreacted hydrogen peroxide using spectrophotometry [13].

2.3 Synthesis of Different Phases Iron Oxide Nanoparticles by Photo Irradiation Method (Photolysis)

In this experiment, the iron salts and complexes, which served as the foundation for the iron oxide nanoparticles, were subjected to radiation within a cell. An immersed UV source, specifically a 125-Watt mercury moderate pressured lamp, was chosen for this purpose. The lamp emits radiation with the highest intensity at a wavelength of 365 nm [15].

By solubilizing 0.6 g of iron III nitrate in 20 mL of water and adding the citric acid solution for the manufacturing of γ-Fe_2O_3 NPs, and 0.84 g of urea with 1.21 g of $Fe(NO_3)_3$ in 10 mL of deionized water for the synthesis of α-Fe_2O_3 NPs, the following instructions were applied for both of solutions, separately. The mixture was agitated for 30 min at 40 °C. The mixture is then exposed to photocell radiation for 30 minutes while being chilled to 5 °C. After obtaining a yellow-brown precipitate of iron (II) complex, the material is filtered and repeatedly cleaned with acetone and deionized water. The precipitate is calcined at 450 °C for 3 hours after being dried in an oven at 60 °C for 4 hours. The result is a reddish-brown magnetic precipitate (γ-Fe_2O_3) [14].

2.4 Characterization techniques

The absorption spectra and λ_{max} of the various phases of iron oxide nanoparticles in different solvents were recorded using the UV-Visible Spectrophotometer at Al-Mustansiriyah University. The morphology of the prepared iron oxide nanoparticles in different phases was examined using a Scanning Electron Microscope (SEM) at Ferdowsi University in Iran.

Scanning Electron microscope (SEM) is used to study the morphology of the prepared different phases of iron oxides nanoparticles at Ferdowsi University - Iran.
X-ray diffraction (XRD) is non–destructive techniques that used to determine the crystalline phase of all synthesized materials at Ferdowsi University - Iran.
Transmission Electron Microscope (TEM) is used to study the morphology, crystal structure and phases of the prepared different phase iron oxides nanoparticles at Cairo University-Egypt.

2.5 Evaluation colloidal solution of Fe_2O_3-NPs in deferent solvents

Before determine the biological activity of α- and γ-Fe_2O_3-NPs, the suitable solvent had been chosen from different selective organic solvents (isopropanol, ethanol, chloroform) in ratio 2.5:2.5 of solvent and water. Three experiments were conducted to determine the appropriate solvent mixture: First: The suitable solvent mixture for Fe_2O_3-NPs was determined by dissolving 0.005 mg of α- and γ-Fe2O3-NPs in 5 mL of each solvent mixture, followed by measuring the λmax using a UV-Visible spectrophotometer. Second: The impact of each solvent mixture individually on catalase (CAT) activity was assessed. Third: The influence of the two phases of Fe_2O_3-NPs, namely α- and γ-, in each solvent mixture on catalase activity was determined.

2.6 Determination the effect of two phases of Fe_2O_3-NPs on catalase activity

A stock solution (0.005M) of α - and γ-Fe_2O_3-NPs in Table 1 has been prepared and then different concentrations (0.005, 0.004, 0.002, 0.001, 0.0005, 0.00025) M of each Fe_2O_3-NPs were prepared by diluting it with the chosen solvent (water). CAT activity was measured in human saliva as follows:

A 450 µL of H_2O_2 + 50 µL of each Fe_2O_3-NPs (each with series of concentrations) were added to 50 µL of salivary sample, through mixing of 5 healthy individuals and 5 pateints. The total salivary activity of CAT was compared under the identical conditions with and without Fe_2O_3-NPs which allowed the calculation of the inhibition percentage.

2.7 Determination the type of inhibition

A fixed level of Fe_2O_3-NPs (lower and higher inhibition) was used with a series of H_2O_2 concentrations (0.01, 0.02, 0.04, and 0.06 M) to explore the type of inhibition. The method was followed as describe in the previous section. The Linewer-Burk formula was used to compare the enzymatic activity with and without the inhibitors, and the values Ki, apparent Vmax (Vmapp), apparent Km (Kmapp), and type of inhibition were computed.

2.8 Docking Study

Molecular docking studies were conducted utilizing the Molegro Virtual Docker 6.0 tool to predict the favored binding mode and binding sites of Fe_2O_3 with catalase (CAT). The structure of Fe_2O_3 was generated using ACD/Chem Sketch. The crystal structure of CAT (PDBID: 1DGH) was obtained from the Protein Data Bank, and its energy was minimized using SPDBV-Swiss-pdb viewer.

2.9 Statistical Analyses

A statistical analysis was carried out by using the student t-test and correlation study by the Pearson-test. Mean results of ±SD and P-to-0.05 have been found. The measurements of mean±SD were carried out using the student t. P for 0.05 was described as statistically significant.

3. Results and Discussion

3.1 Catalase activity in All Studied Groups

The catalase (CAT) levels in the serum and saliva of patients with chronic periodontitis were reported as (mean±SD) in comparison to the control group, as shown in Table 1.

Table 1: Catalase activity (pg/mL) in all patients compared to normal group.

Groups	No.	Mean ∓ SD	Probability
Serum CAT controls	28	63.166∓14.427	0.001
Serum CAT patients	60	83.225∓22.343	
Salivary CAT controls	28	57.355∓18.811	0.002
Salivary CAT patients	60	88.574∓25.210	

The results in Tables 2 indicated that the catalase levels were raised in both gender patients groups compared to control and CAT activity was significantly higher in males than females group, from these results, can conclude that males are more suitable to have periodontitis than females.

Table 2: Gender specific-CAT activity (kU/L) in chronic periodontitis patients and the control.

Gender	Males			Females		
Group	Patient, N=43	Control, N=15	P ≤0.05	Patient, N=16	Control, N=15	P ≤0.05
CAT saliva	89.12±28.75	62.46±30.45	0.001	85.12±35.02	66.57±27.46	0.002
CAT serum	73.20±19.29	68.41±26.65	0.001	73.46±15.96	52.60±17.45	0.002

N: number, kU/L: kilounit per liter.

The human body employs a range of antioxidant defense mechanisms, both enzymatic and nonenzymatic, to eliminate reactive oxygen species and mitigate their detrimental effects on the body. Catalase is a key antioxidant enzyme that plays a vital role in protecting tissues from oxidative damage and regulating the inflammatory response by neutralizing oxygen free radicals generated during various metabolic processes. Antioxidant molecules are present in all tissues and body fluids, serving to counteract the harmful effects of oxidative stress. Catalase scavenges H_2O_2 by converting it to oxygen and water [15]. Previous studies have documented decreased salivary antioxidant ability and increased oxidative damage in the oral cavity associated with periodontal disease [16]. Punj *et al.* [15] found both of serum and salivary

catalase concentrations were lower in disease groups of chronic periodontitis as compared to healthy controls. Dahiya *et al.* [17] and Thomas *et al.* [18] agreed with the results of this study.

The findings of this study contrast with studies carried out by Moore *et al*. [19] and Chapple *et al*. [20] which showed no significant differences in antioxidant concentrations in patients with periodontitis as compared to control groups. These contradictions with our results can be explained by the differences in the systematic methodologies that have been used in the study including sample collection, behavioural condition of the patients as we excluded those who receive an exogenous supplement of antioxidants, and the ethnicity and environmental effects. Chemically, iron nanoparticles can be formed by reducing iron organic or inorganic salt or by reducing iron oxide [21, 22]. In the present work α and γ-IONs was prepared by using photo irradiation cell, the formation of Fe_2O_3-NPs was confirmed by a change of color during the addition of reducing agents (Figure 1).

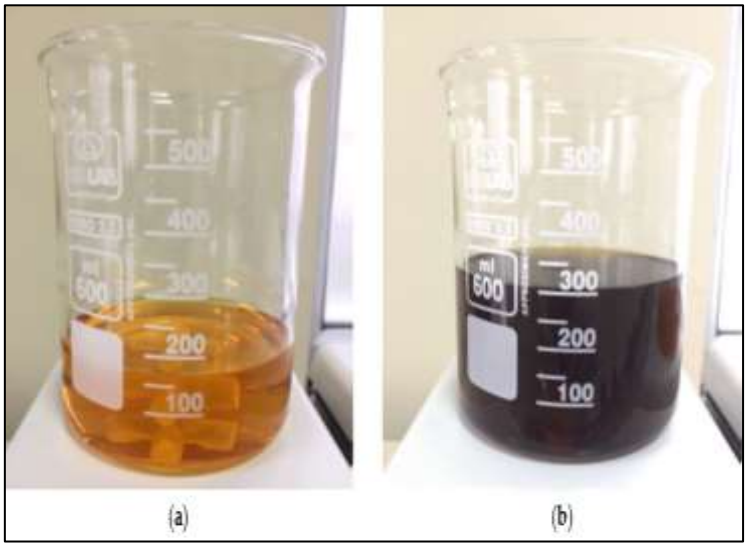

Figure 1: The precursor and product of iron. (**a**) Ferric nitrate precursor salt before photolysis (**b**) Iron nanoparticle formed after photolysis

The functional groups structure include hydroxyl, carboxyl and amino in urea and citric acid can be used act as efficient metal-reducing agents and capping agents in order to provide a protective coating on the metal nanoparticles in a single step, leading to a change in color of Fe_2O_3-NPs as following equations:

3.2 The Mechanism of Iron Nanoparticle Oxidation

The metal core (Fe^0) oxidation is occurred by water. Fe^{2+} and Fe^{3+} are generated in order by the oxidation of Fe^0 (1) and (2). $Fe(OH)_3 \downarrow$ precipitates on the surface of the iron metallic core (3). Dehydrated to oxyhydroxide (FeOOH) (4).

$$2Fe^0_{(s)} + 2H_2O_{(l)} \rightarrow 2Fe^{2+} + H_{2\,(g)} + 2OH^-_{(aq)} \quad \text{……..……..(1)}$$

$$2Fe^{2+} + 2H_2O_{(l)} \rightarrow 2Fe^{3+} + H_{2\,(g)} + 2OH^-_{(aq)} \quad \text{…… (2)}$$

$$2Fe^{3+} + 3OH^- \rightarrow Fe(OH)_3 \downarrow \quad \text{……..(3)}$$

$$Fe(OH)_3 \rightarrow FeOOH \downarrow + H_2O \quad \text{…… …...……(4)}$$

$$FeOOH \rightarrow Fe_2O_3 + H_2O \quad \text{…… ……(5)}$$

The dark color of the obtained Fe_2O_3-NPs was assigned to the plasmon surface resonance of nanosized iron oxide. This interpretation was supported by the appearance of the absorption bands of the spectrum around 217 nm and around 283 nm for γ-Fe_2O_3-NPs and α-Fe_2O_3-NPs, respectively. The mechanism by which Fe_2O_3-NPs are formed is through two successive steps, where in the first the iron slats were complexed in the solution, then in the second, the reducing agents in the solution enables the capping of iron. These findings are in line with the data from previous report by Demirezen *et al.* [23]. The magnetic properties of the Fe_2O_3-NPs have been confirmed towards aggregation the magnetic bar. Iron is nontoxic, inexpensive, biocompatible, and easy to prepare in these types [23].

3.3 UV-Visible Spectroscopy

By monitoring the absorbance of Fe_2O_3-NPs using a UV-Vis spectrophotometer spanning the wavelength range of 200 to 800 nm, the production of these particles has been significantly enhanced. For synthetic - and -iron oxide nanoparticles, the absorption peaks were at 225 nm (Figure 2). These observations are consistent with those of Demirezen *et al.* [23] who described the synthesis of Fe_2O_3-NPs displayed the sharp peak at 205 nm in UV–Vis range. Due to the stimulation of surface plasmon resonance in the Fe_2O_3-NPs mixture, an absorption peak was seen between 200 and 300 nm regions, which is equivalent to the properties of Fe_2O_3-NPs ' UV-visible spectrum [24].

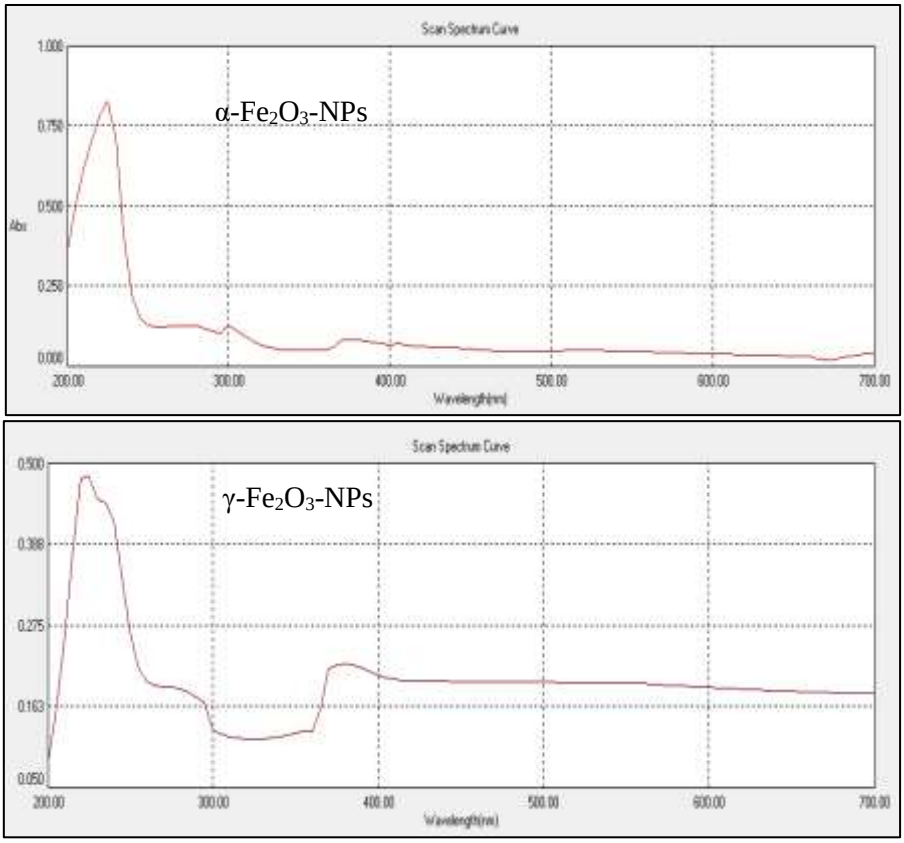

Figure 2: UV-Vis of 0.005mg α- and γ-Fe_2O_3 in 5mL of water

3.4 Scanning Electron Microscopy

The morphological structure of Fe_2O_3-NPs was examined using SEM at different magnification settings (Figure 3). The results showed that the produced Fe2O3-NPs exhibited an aggregated morphology, appearing as asymmetrical cubic and globular forms with rough surfaces. The SEM images clearly depict the formation of nanoparticle clusters or aggregates.

The aggregation of Fe_2O_3-NPs, which probably formed as a consequence of the magnetic dipole-dipole interactions, is clearly visible in the acquired SEM images. Similar occurrences were documented in earlier research [22]. According to the SEM image, nanoparticles have a primary particle size of around 26.8 nm. Urea and citric acid molecules in the test specimen have an impact on the nanoparticles' morphology, causing the cube-shaped nanostructures to develop.

3.5 X-ray Diffraction

The X-ray diffraction (XRD) patterns of Fe_2O_3-NPs are presented in Figure 4. The absence of distinct diffraction peaks in the XRD patterns suggests that the iron nanoparticles were intentionally produced in an amorphous state. This finding aligns with the observations made by Nadagouda et al., [25] and Njagi *et al.* [26] further supporting the amorphous nature of the manufactured iron nanoparticles. It is noticed that the solid diffraction peaks that indicate the crystallinity of Fe_2O_3-NPs exit correspond the JCPDS cards No. 39-1346 and No. 89-4319 for Fe_2O_3-NPs, in which a strong diffraction peaks with 2θ values of 28.26º, 32.28º corresponding to the hkl value of 220, 222, that denotes crystalline phase. The average particle size has been determined by calculating via the Debye-Scherrer formula, which establishes a correlation of peak broadening in XRD and particle size. The Scherrer formula is used to estimate the mean crystallite sizes of Fe_2O_3-NPs, which are found to be between 14 and 26 nm. The outcomes showed that all of the nanoparticles were in face-centered cubic spinel form.

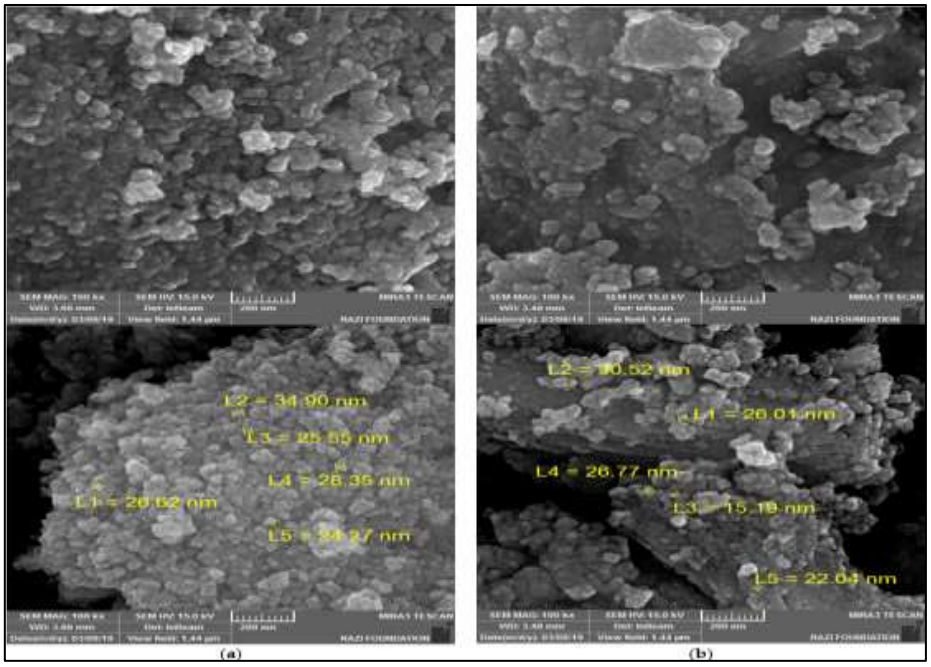

Figure 3: The SEM images for Iron oxide nanoparticles. (**a**) α-Fe_2O_3; (**b**) γ-Fe_2O_3

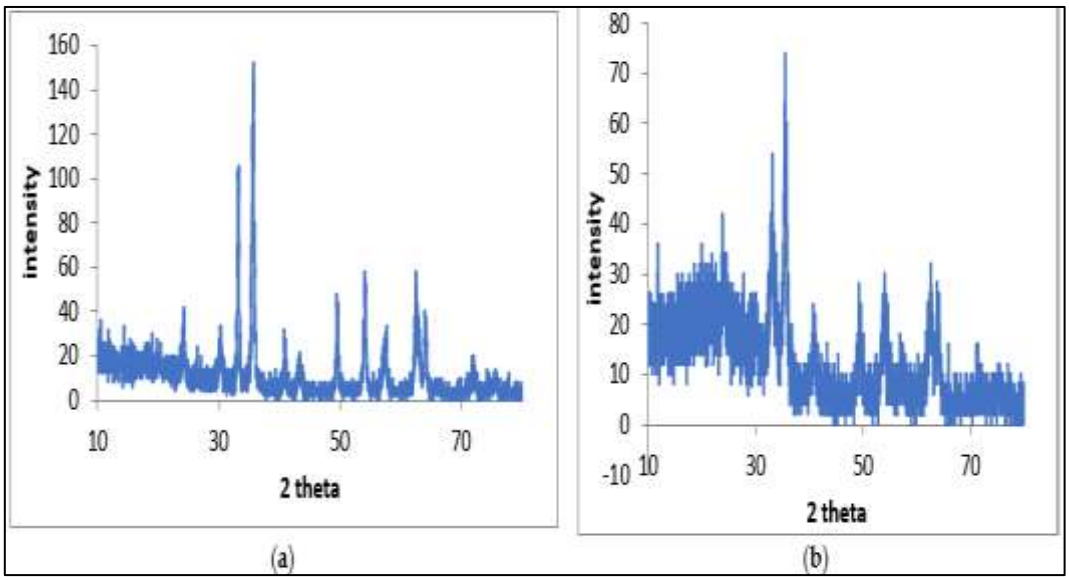

Figure 4: XRD pattern of Iron oxide nanoparticles. (**a**) α-Fe_2O_3; (**b**) γ-Fe_2O_3

3.6 *In Vitro* kinetic Study

Some of the latest works have shown the ability of Fe_2O_3-NPs for remediating the environment. Nanoadsorbents, nanocatalysts, nanofiltration or nanobiocides are widely used for the treatment of water and waste water contaminants. Among these species, Fe_2O_3-NPs have demonstrated potential improvements in combating environmental pollution. The sensitivity of iron in its nanoscale with such a high ratio of surface area to volume is increasing the interest in environmental rehabilitation using nanoscale zero-valent iron [21]. Fe_2O_3-NPs interactions lead to additive, synergistic or inhibitory effects on the function of the enzymes. Butoxidase, lysozyme, lactoferin and histatins are the major innated oral defense factors. Catalase is an enzyme that is secreted from mammary, salivary and other glands of the mucosa that acts as a natural antibacterial [27].

Recent nanomaterial advances offer a new method for regulating protein behavior by surface interactions. The enzyme was less stable on the surface of nanoparticles than in the free solution, and the stability of larger particles with smaller surface curvature was further decreased. Although most native structure of protein may be retained after adsorption on the surface of the NPs. In some cases the protein's thermodynamic stability is reduced allowing the protein more sensitive to chemical denaturants like urea [28].

3.7 The Optical Properties of Iron Oxide Nanoparticles in Different Solvents

To determine the most suitable solvent for the kinetic study of the catalase enzyme, the solubility of nanoparticles in various solvents was initially assessed. A ratio of 2.5:2.5 of each solvent with water was prepared, and the λ_{max} (maximum absorbance wavelength) was measured. This investigation aimed to identify the solvent that demonstrated the highest solubility and compatibility for conducting the kinetic study of the catalase enzyme.

As shown in Figure 2 by using water as solvent and Figure 5 by using organic solvents, the most suitable solvent is the water according to λ_{max} (abs : 0.484 at 225 nm and abs : 0.829 at 225) for γ-Fe_2O_3 and α-Fe_2O_3, respectively .In addition ,the effect of each solvents on salivary catalase activity was tested and appeared that water as a solvent has little effect on enzyme activity than other solvents which showed inhibit on catalase activity, as well as enzyme activity was experimented again with α -and γ- iron nanoparticles which was dissolved in each solvents, results indicated that iron nanoparticles in water is the perfect for kinetic enzymatic study.

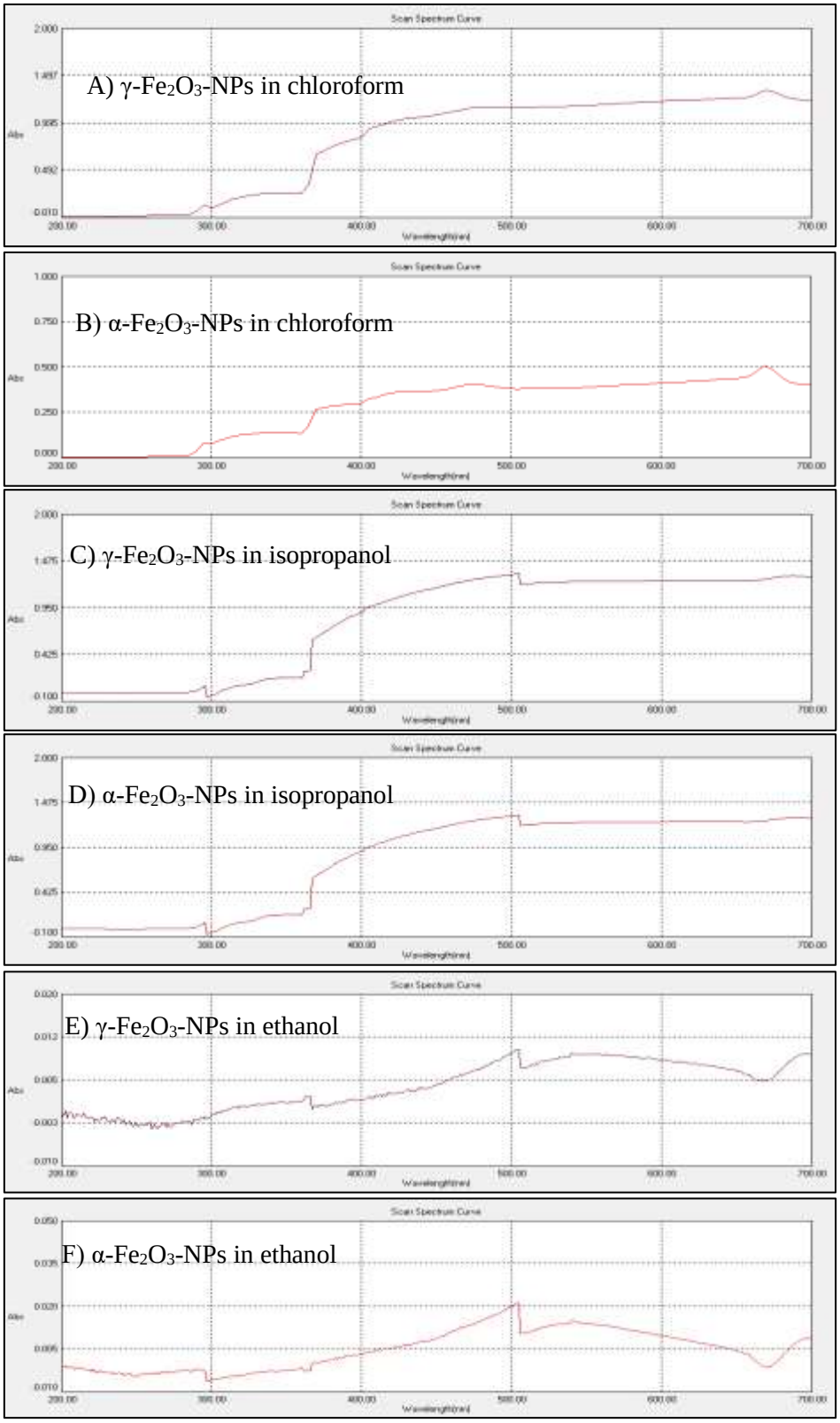

Figure 5: UV-Vis of α- and γ-Fe_2O_3 in different solvents. **A)** γ-Fe_2O_3-NPs in chloroform, **B)** α-Fe_2O_3-NPs in chloroform, **C)** γ-Fe_2O_3-NPs in isopropanol, **D)** α-Fe_2O_3-NPs in isopropanol, **E)** γ-Fe_2O_3-NPs in ethanol, **F)** α-Fe_2O_3-NPs in ethanol

3.8 TEM analysis

Morphologies of the nanoparticles that form as dispersion solution in water were confirmed by employing TEM analysis shown in Figure 6. The mean size of the globular nanostructured

materials made out of colloidal Fe_2O_3-NPs in water was 20 nm, and the granules were observed to be agglomerated. Correspondingly, Makarov *et al.* [29] TEM examination of Rumex acetosa revealed the formation of documented electron-dense amorphous particles measuring up to 40 nm in size. On the other hand, Hordeum vulgare extracts resulted in the production of electron-dense sphere-shaped Fe_2O_3-NPs, with a maximum size of 30 nm, as observed by TEM.

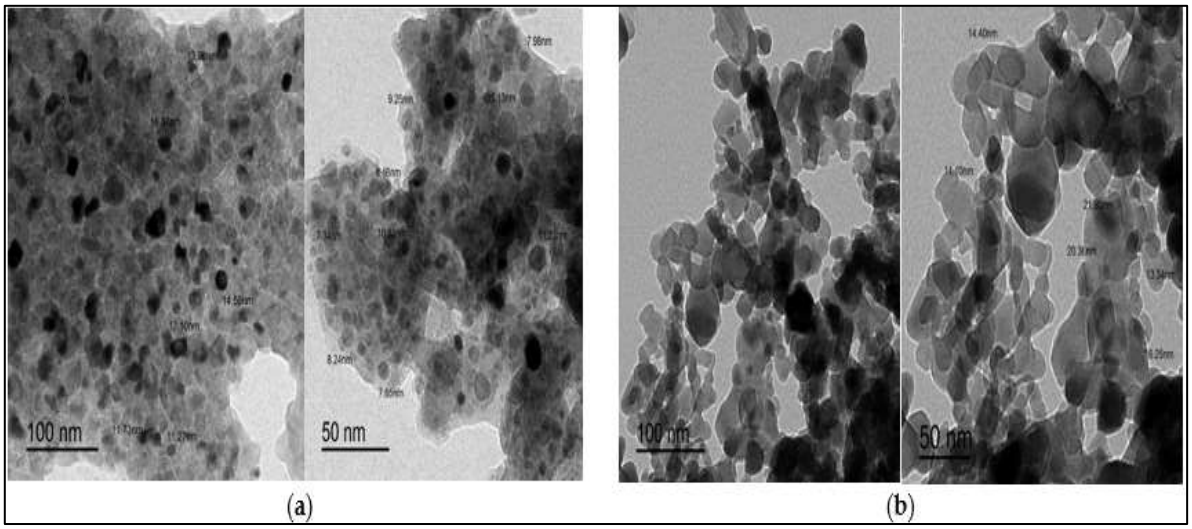

Figure 6: TEM for Iron oxide nanoparticles. (**a**) α-Fe_2O_3; (**b**) γ-Fe_2O_3

3.11 The effect of colloids iron oxide nanoparticles solution on salivary catalase activity in chronic periodontitis patients and healthy samples (*in vitro* study)

Fluorescent biological labeling, drug and gene delivery, biodetection of infections, and peptide detection are some of the key uses of nanostructured materials in biomedical science. DNA structural analysis, tissue engineering, heating (hyperthermia) to destroy tumors, and separating and purifying biomolecules and cells are some of the techniques used [30].

Present study examined the *in vitro* effect of two-phase iron oxide Nanoparticles (α-Fe_2O_3 and γ -Fe_2O_3) on the salivary catalase activity in patients and healthy subjects. Human catalase activity was measured in the presence of different α- and γ-Fe_2O_3-NPs concentrations as presented in Table 3 and Table 4.

Table 3: The effect of α-Fe_2O_3-NPs on CAT activity in periodontitis patients and normal group

Samples	Inhibitor con. (M)	CAT activity (kU/L)	% Inhibition
Healthy control	zero	65.17	-
α-Fe_2O_3 in healthy sample	2.5×10^{-4}	48.13	26.14
	5×10^{-4}	51.17	21.48
	10^{-3}	29.75	54.35
	2×10^{-3}	26.76	58.93
	4×10^{-3}	52.31	21.48
	5×10^{-3}	18.01	72.36*
Patient control	zero	101.2	-
α-Fe_2O_3 in patient sample	2.5×10^{-4}	92	9.09
	5×10^{-4}	90.25	10.82
	10^{-3}	63.08	37.66
	2×10^{-3}	59.87	40.83*
	4×10^{-3}	81.31	19.65
	5×10^{-3}	80.76	20.19

kU/L: kilounit per liter.

Table 4: The effect of γ-Fe_2O_3-NPs on CAT activity in periodontitis patients and normal group

Samples	Inhibitor con. (M)	CAT activity (kU/L)	% Inhibition
Healthy control	zero	65.17	-
γ-Fe_2O_3 in healthy sample	2.5×10-4	32.71	63.61
	5×10-4	7.54	88.43*
	10-3	23.27	64.21
	2×10-3	36.74	43.62
	4×10-3	55.53	14.79
	5×10-3	59.75	8.31
Patient control	zero	101.2	-
γ-Fe_2O_3 in patient sample	2.5×10-4	83	19.35
	5×10-4	54.73	54.81
	10-3	10.10	90.01*
	2×10-3	12.57	87.57
	4×10-3	65.54	35.23

kU/L: kilounit per liter

The activity of the control cuvette, in the absence of the inhibitor, was verified to be 100%. To determine the kinetic constants, six different levels of Fe_2O_3-NPs (0.005 M, 0.004 M, 0.002 M, 0.001 M, 0.0005 M, and 0.00025 M) were tested for each specimen.

The biochemical tests indicated that two phase Fe_2O_3-NPs have demonstrated an inhibitory influence on CAT activity in each of the two groups (healthy and patients) compared to the values of the standardly evaluated activities of CAT which were 17 kU/L in healthy control and 101.2 kU/L in periodontitis patients. The two parameters of Fe_2O_3-NPs inhibited the activity of the enzyme in a graded manner from low to intermediate levels until reaching an elevated doses of Fe_2O_3-NPs which showed a modest inhibitory effect on CAT activity. Increasing CAT activity in saliva of periodontics patient compare to healthy group can be attributed to the role of CAT in control the level of H_2O_2 secreted by bacteria and leukocyte cells which lead to specific antibacterial activity by inhibition the metabolism of proliferation of various bacteria in the oral cavity [30].

Table 3 and Table 4 concluded that the inhibition percentages % are (72.36%, 40.33%) in healthy and patient samples that incubated with α-Fe_2O_3-NPs at concentrations ($5x10^{-3}$, $2x10^{-3}$) M, respectively, at the same time, are (88.43%, 90.01%) in in healthy and patient samples that incubated with γ-Fe_2O_3-NPs at concentrations ($5x10^{-4}$, $1x10^{-3}$) M respectively.These are attributable to the presence of a space for Fe_2O_3-NPs which could lead to good orientation of active site gorge of enzyme and upon entering the heme cavity, is severely sterically hindered and lead to interact with histidine (His74) and asparagine (Asn14) residues that are important for binding and interactions of the inhibitors at these concentrations and fit into the active site easily or may due to interact of Fe_2O_3-NPs to another sites on enzyme that lead to inhibition [31].

Results concluded that, the reason of CAT inhibition is heavy metals (Fe_2O_3-NPs) that can interact with protein, so they bind protein molecules. Heavy metals inactivate the enzymes by interact strongly with thiol groups in these enzymes. These findings are in agreement with Chudasama *et al.* [32]. Also, it is came up to believe that iron binds to functional groups of proteins resulting in protein deactivation and denaturation. This fact is in agreement with Raffi *et al.* [33]. The current study hypothesizes that Fe_2O_3-NPs inactivate the CAT by intraction with functional groups of amino acid in enzyme resulting in protein denaturation, and as a conclusion the Fe_2O_3-NPs inhibited the enzyme. It was not easy to compare our work with other

studies exactly because, in our knowledge, this is the only study to show the effect of Fe_2O_3-NPs solution on total activity of salivary catalase enzyme.

A further reason for Fe_2O_3-NPs behavior could be assigned to the torsional variations in the tertiary or quaternary CAT protein structure. The secondary structure of the enzyme was changed by Fe_2O_3-NPs with changes in α helix and β sheet content. In addition, the α-helix content decreased as the β sheet content increased, resulting in a loss of activity [34]. Yu *et al.* [34] found that super-paramagnetic iron oxide nanoparticles (SPIONs) can interact with proteins to alter the structure and function of the catalase enzyme. UV–vis spectroscopy data showed that CAT α-helical content in the presence of SPIONs decreased from 32.4 % to 29.1 %. In addition, in presence of SPION at a 20:1 particle: protein ratio 10% decrease in CAT activity was observed.

In addition, catalase was found to fit the Michaelis – Menten kinetic model, and the existence of inhibitor Fe_2O_3-NPs did not affect the enzyme's hyperbolic saturation behavior. The effect of maximum and minimum concentrations of Fe_2O_3-NPs in each group (patients, healthy) at different hydrogen peroxide concentrations (0.01, 0.02, 0.04, 0.06) M on catalase activity was observed. It is critical to understand how Fe_2O_3-NPs bind with proteins and how this binding inhibits the function of CAT. Future research should concentrate on the protein modifications produced by Fe_2O_3-NPs. As a result, several investigations are required to elucidate this connection. All of the above results are in a good agreement with previous studies [37-41]. Lineweaver –Burk graph showed that (α-Fe_2O_3 and λ-Fe_2O_3) inhibit catalase by different types of inhibition and gave different Ki values. All above results were summarized in Tables 5 and 6.

Table 5: The kinetic parameters of catalase with and without α-Fe_2O_3 nanoparticles in saliva of healthy and periodontics subjects

Sample	Inhibitor Conc.(M)	Km (M)	Vmax (KU/L)	Ki (M)	Inhibition type
Healthy Control	Zero	0.033	66.66	-	-
α-Fe_2O_3 in healthy sample	5×10^{-3}	0.011	33	4.72×10^{-2}	Un-competitive
	5×10^{-4}	0.011	16.6	1.59×10^{-4}	Un-competitive
Patient Control	Zero	0.015	76.92	-	-
α-Fe_2O_3 in patient sample	2.5×10^{-4}	0.025	66.66	2.71×10^{-4}	Mix
	10^{-3}	0.033	55.55	4.9×10^{-4}	Mix

Km: Michaelis-Menten constant, Vmax: maximum velocity, Ki: inhibition constant.

Table 6: The kinetic parameters of catalase with and without α-Fe_2O_3 nanoparticles in saliva of healthy and periodontics subjects

Sample	Inhibitor Conc.(M)	Km (M)	Vmax (kU/L)	Ki (M)	Inhibition type
Healthy	Zero	0.033	66.66	-	-
γ-Fe_2O_3 in healthy sample	4×10^{-3}	0.033	11.76	8.57×10^{-4}	Non-competitive
	5×10^{-3}	0.025	28.57	3.67×10^{-4}	Un-competitive
Patient Control	Zero	0.015	76.92	-	-
γ-Fe_2O_3 in patient sample	2.5×10^{-4}	0.015	68.96	2.16×10^{-3}	Non-competitive
	2×10^{-3}	0.013	65.35	1.12×10^{-2}	Un-competitive

Km: Michaelis-Menten constant, Vmax: maximum velocity, Ki: inhibition constant.

From this presentation the study indicated that Km was varied from high, same or less in the presence of Fe_2O_3-NPs compared with non- inhibiting system. The highest values of Km were obtained upon the use of α-Fe_2O_3-NPs in periodontitis group at a concentration of 10^{-3} M which indicated a complex inhibition effect. On other hand, γ-Fe_2O_3-NPs exhibited the higher Km value at 2.5×10^{-4} M on the activeenzyme site which did not compete with H_2O_2; therefore, exhibiting a noncompetitive inhibition effect. α-Fe_2O_3-NPs at (5×10^{-3}, 5×10^{-4}) M and γ-Fe2O3-NPs at ($5x10^{-3}$ M, $2\ x10^{-4}$ M) showed low Km value that mean a higher affinity of substrate toward enzyme gorge (uncompetitive inhibition). Conclusively, various variables influence affinity, including size, three-dimensional configuration, the concentration of Fe_2O_3-NPs, which easily interacts, non-covalently, to groups inside or around the active site, along with other factors. Tables 5 and 6 showed that the Vmax values for the untreated samples (66.66 and 76.92 kU/L) were higher in both the healthy and patient samples than in the inhibited samples. So, it is evidenced that the number of active sites were higher in untreated samples than those in the samples that were treated with the two types of Fe_2O_3-NPs.
Since the data are consistent with the kinetics of the tight-binding inhibition, strong inhibition, and all assumptions underpinning the traditional Michaelis-Menten models are being verified, it is plausible to draw this conclusion from the differential Ki values. Additionally, the results demonstrated that Fe_2O_3-NPs display various forms of inhibition at both their highest and lowest concentrations. The configuration of inhibitors that undergo structural modifications after attaching to the imidazole group of Asn, His in CAT, which is either situated in the catalytic site or crucial in defining the active conformation of the enzyme molecule, can be used to characterize mixed inhibition. Conversely, un- and non-competitive inhibition may be described by using the traditional theories, which propose that the inhibitor attaches to a different place on the enzyme, changing its conformation to lock the enzyme and inhibit the binding of the substrate or reducing CAT affinity. Catalase showed inhibition constant Ki in the range (10^{-2} -10^{-5}) M in presence of maximum and minimum Fe_2O_3-NPs (inhibitors) concentrations, which is probably due to variant type of inhibition from mix, non- and uncompetitive.

The inclusion of Fe_2O_3-NP inhibitors lowers the enzymatic reaction's Vmax without changing the Km (unaffected), demonstrating that the inhibitor binds to both unbound catalase and catalase-H_2O_2 ensembles equally effectively. The particular active location where H_2O_2 substrate is located is not where this interaction event is most likely to take place entirely. As a result, Fe_2O_3-NPs appear to be a typical non-competitive inhibitor, while being infrequent in practice.

A further indication that the inhibitor of Fe_2O_3-NPs binds effectively to a different location on unbound catalase is the fact that their presence lowers the maximum rate Vmax of enzymatic reactions with and without affecting the Km. In light of this, it appears that Fe_2O_3-NPs is a classic mix-competitive inhibitor, albeit being infrequent in reality.

The existence and growth of microbial cells in the body are referred to as infections. Periodontal disease is a series of conditions caused by specific bacteria present in subgingival plaques that affect the gum and tooth support systems (ligament and alveolar bone). The most important and most prevalent anaerobic gram-negative bacteria in the subgingival area are *Actinobaci-llus actinomycetemcomitans* (Aa), *Porphyromonas gingivalis* (Pg), *Prevotella intermedia* (Pi), *and Tannerella forsythensis* (Tf). Through an immunopathogenic process, these bacteria contribute significantly to the start and progression of periodontitis by helping to create the periodontal pocket, destroy soft tissue, and resorb alveolar bone [35]. In tissues, antioxidant enzymes such catalase, glutathione peroxidase, and superoxide dismutase play a role in cellular anti-oxidative processes. H_2O_2, a highly reactive oxygen species, contributes to

the pathophysiology of several illnesses. The enzymatic antioxidants catalase, which is present in several types of cells, is thought to be crucial in the elimination of H_2O_2. This molecule can shield DNA and cellular membranes from the harmful oxidization by accelerating a step that breaks down harmful H_2O_2, which is formed as a consequence of many typical cellular activities, and decrease of catalase function is linked to an increased sensitivity to oxidative stress, hence this activity is crucial for cells [36].

The inhibitory effects of Fe_2O_3-NPs were only established in the current experiment during incubations of varied specific doses of the inhibitor with catalase. These circumstances are conceivable and typical of physiological levels, and the reported inhibition is probably the result of using Fe_2O_3-NPs as an orthodontic filler. At first, low Fe_2O_3-NP inhibition percentages had little impact on catalase activity, which in turn, lowers the production of reactive oxygen species (ROS).
Furthermore, a high inhibitory percentage of Fe_2O_3-NPs in CAT results in the production of free radicals, which can result in apoptotic cell death and necrosis of bacterial and infectious cell populations by the buildup of H_2O_2. [37]. It was discovered that the concentration and dimension of the nanomaterials affect the impact of Fe_2O_3-NPs on the antioxidant enzyme catalase activity. Specific nanoparticles concentrations that significantly altered the catalase function which might produce a buildup of hydrogen peroxide, which is harmful to bacterial cells. The results are in a good agreement with Usatîi *et al*. [38].

Although the precise method by which Fe_2O_3-NPs reduce CAT activity is unclear, a straightforward explanation could be used. Given that CAT is a protein and possesses an amine and a carboxyl group at its N- and C-termini, correspondingly, conjugation to these peptides might take place at either of these locations. It is possible that this contact makes the enzyme inaccessible to the substrate [39].

The water attached to His75 and Asn148, whose only active site residues other than the heme that associate with the inhibitor in the human catalase molecule, suggests that competing with H_2O_2 is primarily for Fe_2O_3-NPs interaction [40]. Nevertheless, several investigations found that a number of substances, including catalase's natural substrate H_2O_2, azide, acetic, formic, fluoride, cyanide, hydroxylamine, carbon monoxide, heavy metals (Cu^{2+}, Pb^{2+}), and 3-amino-1,2,4-triazine, impede its action [41].

It has been established that ROS are harmful but also serve as chemical messengers. The ability of contaminated cells in periodontitis to resist intercellular ROS signals is mediated by the production of catalase on the cell membrane. By supplying H_2O_2 and inhibiting catalase, infected cells' intercellular ROS signaling can be recovered. These results establish the molecular underpinnings of selective induced apoptosis in bacterial and infected cells, and they provide an unique strategy for the treatment and control of inflammation. It has been postulated that the catalase enzyme may have a function in the genesis of cancer based on prior research that demonstrated that aggressive lung tumors had drastically lower enzymatic activity. Catalase may have several impacts on cancerous cells and may slow tumor growth by altering the intracellular redox state, but mesothelioma cells' increased antioxidant capacity may also shield tumor cells from external oxidants. Catalysts play a crucial role in biology because they significantly speed up the rate at which ordinary chemical processes take place. Without catalase, vital processes would require days or months to complete, and the body's poisonous H_2O_2 would build up very fast [36]. It is a crucial enzyme in preventing ROS-induced oxidative cell damage. Drugs attach to enzymes and cause enzyme inhibition. Catalase inhibition by wogonin, for instance, caused H_2O_2 buildup and cytotoxicity in bacterial cells via activating apoptosis and H_2O_2 [39]. Another research that was used to support this one showed that

hydrogen peroxide is harmful to the microorganisms that cause periodontal disease and that sodium bicarbonate and hydrogen peroxide work together synergistically to kill those germs [41]. By lowering the amount of germs in the mouth and aiding in the infection's clearance, hydrogen peroxide may reduce pain. By releasing oxygen and altering the habitat of anaerobic bacteria, hydrogen peroxide may aid in the killing of bacteria [42]. Despite extensive research on catalases over the years, there are still many intriguing questions regarding their functioning in the presence of various inhibitors. Important aspects such as the kinetic parameters and the mechanisms of inhibition are yet to be fully understood. Understanding these aspects is crucial, as the activity of catalase can be affected by potential drugs within cells. In the context of infected and bacterial cells, the local application of Fe_2O_3-NPs could be beneficial. The presence of Fe_2O_3-NPs could significantly reduce catalase activity and increase the concentration of H_2O_2 in these cells. This modulation of catalase activity and H_2O_2 levels may have implications for therapeutic approaches targeting infections, as it could potentially enhance the efficacy of treatments by exploiting the inhibitory effects of Fe_2O_3-NPs on catalase activity.

3.12 Docking Results

The best binding energy between CAT and Fe_2O_3 was found to be -41.29 kcal/mol with 2 hydrogen bonds. This value shows high binding affinity for nanoparticle to the protein. The closest interacting residues which can contribute in hydrogen bonding are SER-254A and ARG-127A as shown in Figure 7. The docked structure showed the binding region of CAT-Fe_2O_3-NPs complex being surrounded by the three amino acid residues of CAT including the Thr125, lle205, Ala250.

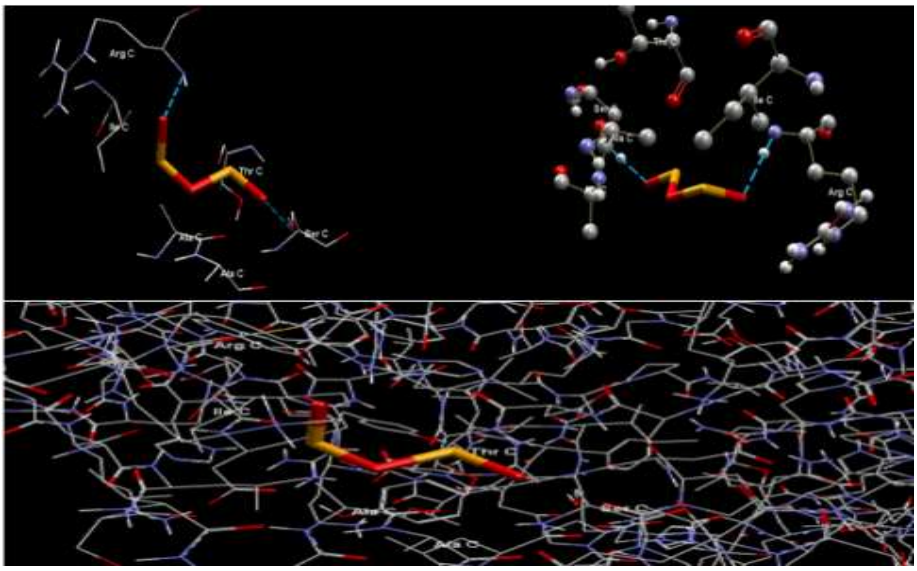

Figure 7: The binding regions of Fe_2O_3-NPs with CAT

4. Conclusion

Despite extensive research spanning several years, numerous intriguing questions regarding the functioning of catalases in the presence of different inhibitors remain unresolved. Key areas that lack clarity include the determination of kinetic parameters and the elucidation of inhibition mechanisms. Despite the wealth of knowledge accumulated, understanding the intricate details of catalase activity in the presence of inhibitors remains a captivating and ongoing pursuit. This is because the activity of catalase can be decreased by possible medicines in cells. As a result, localized administration of Fe_2O_3-NPs as an amalgam might drastically reduce catalase activity and raise the level of H_2O_2, which would have a positive impact on bacteria and infected cells alone.

5. Acknowledgments

The authors express their gratitude to the College of Science at Mustansiriyah University and College of Dentistry at University of Baghdad for their supporting role during this work.

"All experiments followed were in accordance with Helsinki Declaration of 1975, as revised in 2000. An informed consent for all human subjects included in the study is also required. For studies with animals, authors must indicate the following sentence in a section preceding the References: "All institutional and national guidelines for the care and use of laboratory animals were followed."

"Conflict of Interest: The authors declare that they have no conflicts of interest."

References

[1] S. Shrestha, M. Neupane, S. Sharma, and M. Lamsal, "Assessment of tumor necrosis factor-alpha in gingivitis and periodontitis patients", *ried*, vol. 25, pp. 6, 2017.

[2] J. Dufty, N. Gkranias, and N. Donos, "Necrotising ulcerative gingivitis: a literature review", *Oral Health Prev Dent*, vol. 15, no. 4, pp. 321-327, 2017.

[3] L. Abusleme, A. Hoare, B. Y. Hong, and P. I. Diaz, "Microbial signatures of health, gingivitis, and periodontitis", *Periodontology 2000*, vol. 86, no. 1, pp. 57-78, 2021.

[4] K. Edman, K. Ohrn, A. Holmlund, B. Nordström, M. Hedin, and D. Hellberg, "Comparison of oral status in an adult population 35-75 year of age in the county of Dalarna, Sweden in 1983 and 2008", *Swedish dental journal*, vol. 36, no. 2, pp. 61-70, 2012.

[5] T. Dietrich, P. Ower, M. Tank, N. West, C. Walter, I. Needleman, and British Society of Periodontology, "Periodontal diagnosis in the context of the 2017 classification system of periodontal diseases and conditions–implementation in clinical practice", *British dental journal*, vol. 226, no. 1, pp. 16-22., 2019.

[6] K. Eriksson *et al.*, "Seropositivity combined with smoking is associated with increased prevalence of periodontitis in patients with rheumatoid arthritis", *Annals of the rheumatic diseases*, vol. 77, no. 8, pp. 1236-1238, 2018.

[7] Y. Aksoy, M. Balk, H. ÖĞÜŞ, and N. Özer, "The mechanism of inhibition of human erythrocyte catalase by azide", *Turkish Journal of Biology*, vol. 28, no. 2-4, pp. 65-70, 2005.

[8] S. A. M. Ealia and M. Saravanakumar, "A review on the classification, characterisation, synthesis of nanoparticles and their application", *IOP Conference Series: Materials Science and Engineering*, vol. 263, no. 3: IOP Publishing, p. 032019, 2017.

[9] R. M. Cornell and U. Schwertmann, *The Iron Oxides*. 2003.

[10] A. S. Teja and P.-Y. Koh, "Synthesis, properties, and applications of magnetic iron oxide nanoparticles", *Progress in crystal growth and characterization of materials*, vol. 55, no. 1-2, pp. 22-45, 2009.

[11] C. Xu, O. U. Akakuru, J. Zheng, and A. Wu, "Applications of iron oxide-based magnetic nanoparticles in the diagnosis and treatment of bacterial infections", *Frontiers in bioengineering and biotechnology*, vol. 7, p. 141, 2019.

[12] V. F. Cardoso, A. Francesko, C. Ribeiro, M. Bañobre-López, P. Martins, and S. Lanceros-Mendez, "Advances in magnetic nanoparticles for biomedical applications", *Advanced healthcare materials*, vol. 7, no. 5, p. 1700845, 2018.

[13] L. Goth, "A simple method for determination of serum catalase activity and revision of reference range", *Clinica chimica acta*, vol. 196, no. 2-3, pp. 143-151, 1991.

[14] D. H. Hussain, H. I. Abdulah, and A. M. Rheima, "Synthesis and characterization of ɣ-Fe_2O_3 nanoparticles photo anode by novel method for dye sensitized solar cell", *International Journal of Scientific and Research Publications*, vol. 6, no. 10, pp. 26-31, 2016.

[15] A. Punj, S. Shenoy, N. S. Kumari, and P. Pampani, "Estimation of antioxidant levels in saliva and serum of chronic periodontitis patients with and without ischemic heart disease", *International journal of dentistry*, vol. 2017, pp. 152-159, 2017.

[16] R. Diab-Ladki, B. Pellat, and R. Chahine, "Decrease in the total antioxidant activity of saliva in patients with periodontal diseases", *Clinical oral investigations*, vol. 7, no. 2, pp. 103-107, 2003.

[17] P. Dahiya, R. Kamal, R. Gupta, and H. Saini, "Evaluation of the serum antioxidant status in patients with chronic periodontitis", *Indian Journal of Multidisciplinary Dentistry*, vol. 6, no. 1, p. 3, 2016.

[18] B. Thomas, A. Ramesh, S. Suresh, and B. R. Prasad, "A comparative evaluation of antioxidant enzymes and selenium in the serum of periodontitis patients with diabetes mellitus type 2", *Contemporary clinical dentistry,* vol. 4, no. 2, p. 176, 2013.

[19] S. Moore, K. A. Calder, N. J. Miller, and C. A. Rice-Evans, "Antioxidant activity of saliva and periodontal disease", *Free radical research,* vol. 21, no. 6, pp. 417-425, 1994.

[20] I. Chapple, G. Brock, M. Milward, N. Ling, and J. Matthews, "Compromised GCF total antioxidant capacity in periodontitis: cause or effect", *Journal of clinical periodontology,* vol. 34, no. 2, pp. 103-110, 2007.

[21] S. Saif, A. Tahir, and Y. Chen, "Green synthesis of iron nanoparticles and their environmental applications and implications", *Nanomaterials,* vol. 6, no. 11, p. 209, 2016.

[22] E. Da'na, A. Taha, and E. Afkar, "Green synthesis of iron nanoparticles by acacia nilotica pods extract and its catalytic, adsorption, and antibacterial activities", *Applied Sciences,* vol. 8, no. 10, p. 1922, 2018.

[23] D. A. Demirezen, Y. Ş. Yıldız, Ş. Yılmaz, and D. D. Yılmaz, "Green synthesis and characterization of iron oxide nanoparticles using Ficus carica (common fig) dried fruit extract", *Journal of bioscience and bioengineering,* vol. 127, no. 2, pp. 241-245, 2019.

[24] O. U. I. a. F. Nwamezie, "Green synthesis of iron nanoparticles using flower extract of Piliostigma thonningii and their antibacterial activity evaluation", *Chemistry International,* vol. 4, no. 1, pp. 60-66, 2018.

[25] M. N. Nadagouda and R. S. Varma, "A greener synthesis of core (Fe, Cu)-shell (Au, Pt, Pd, and Ag) nanocrystals using aqueous vitamin C", *Crystal Growth and Design,* vol. 7, no. 12, pp. 2582-2587, 2007.

[26] E. C. Njagi *et al.*, "Biosynthesis of iron and silver nanoparticles at room temperature using aqueous sorghum bran extracts", *Langmuir,* vol. 27, no. 1, pp. 264-271, 2011.

[27] I. Fita and M. G. Rossmann, "The active center of catalase", *Journal of molecular biology,* vol. 185, no. 1, pp. 21-37, 1985.

[28] S. T. Abd and A. F. Ali, "Effect of zinc oxide nanoparticles on total salivary peroxidase activity of human saliva (In vitro study)", *Journal of Baghdad College of Dentistry,* vol. 27, no. 2, pp. 178-182, 2015.

[29] V. V. Makarov *et al.*, "Biosynthesis of stable iron oxide nanoparticles in aqueous extracts of Hordeum vulgare and Rumex acetosa plants", *Langmuir,* vol. 30, no. 20, pp. 5982-5988, 2014.

[30] K. K. Ghudhaib, A. M. I. Leka, E. A. Salman, and Z. A. Salman, "Effect of Zno Nanoparticles on Salivary Peroxidase Activity In Chronic Periodontitis Patients (In Vitro Study)", *IOSR Journal of Applied Chemistry,* vol. 9, no. 4, 2016.

[31] S. Antonyuk *et al.*, "Three-dimensional structure of the enzyme dimanganese catalase from Thermus thermophilus at 1 Å resolution", *Crystallography Reports,* vol. 45, no. 1, pp. 105-116, 2000.

[32] B. Chudasama, A. K. Vala, N. Andhariya, R. Mehta, and R. Upadhyay, "Highly bacterial resistant silver nanoparticles: synthesis and antibacterial activities", *Journal of Nanoparticle Research,* vol. 12, no. 5, pp. 1677-1685, 2010.

[33] M. Raffi, F. Hussain, T. Bhatti, J. Akhter, A. Hameed, and M. Hasan, "Antibacterial characterization of silver nanoparticles against E. coli ATCC-15224", *Journal of materials science and technology,* vol. 24, no. 2, pp. 192-196, 2008.

[34] Z. Yu, H. Liu, X. Hu, W. Song, and R. Liu, "Investigation on the toxic interaction of superparamagnetic iron oxide nanoparticles with catalase", *Journal of Luminescence,* vol. 159, no. 12, pp. 312-316, 2015.

[35] E. F. Ruiz and A. B. Martínez, "Periodontal diseases as bacterial infection", *Avances en periodoncia e implantologia Oral,* vol. 17, no. 3, pp. 111-118, 2005.

[36] S. Islamovic, B. Galic, and M. Milos, "A study of the inhibition of catalase by dipotassium trioxohydroxytetrafluorotriborate K_2 $[B_3O_3F_4OH]$", *Journal of enzyme inhibition and medicinal chemistry,* vol. 29, no. 5, pp. 744-748, 2014.

[37] A. Murali and S. Patel, "The effect of different heavy metal acetate solutions on the inhibition of catalase enzyme", *Journal of the South Carolina Academy of Science,* vol. 15, no. 2, p. 13, 2017.

[38] N. Efremova, "Effect of Fe3O4 and TiO2 Nanoparticles on Catalase Activity and Î²-Carotene Content at Pigmented Yeast Strain Rhodotorula gracilis", *Acta Universitatis Cibiniensis. Series E: Food Technology,* 2017.

[39] S. Pal, S. K. Dey, and C. Saha, "Inhibition of catalase by tea catechins in free and cellular state: a biophysical approach", *PLoS One*, vol. 9, no. 7, p. e102460, 2014.

[40] C. D. Putnam, A. S. Arvai, Y. Bourne, and J. A. Tainer, "Active and inhibited human catalase structures: ligand and NADPH binding and catalytic mechanism", *Journal of molecular biology*, vol. 296, no. 1, pp. 295-309, 2000.

[41] M. V. Marshall, L. P. Cancro, and S. L. Fischman, "Hydrogen peroxide: a review of its use in dentistry", *Journal of periodontology*, vol. 66, no. 9, pp. 786-796, 1995.

[42] T. N. Phan, A. Kirsch, and R. Marquis, "Selective sensitization of bacteria to peroxide damage associated with fluoride inhibition of catalase and pseudocatalase", *Oral microbiology and immunology*, vol. 16, no. 1, pp. 28-33, 2001.